J|A|C|S
ARTICLES
Published on Web 01/14/2004

Synthesis, Structure, Theoretical Studies, and Ligand Exchange Reactions of Monomeric, T-Shaped Arylpalladium(II) Halide Complexes with an Additional, Weak Agostic Interaction

James P. Stambuli,[†] Christopher D. Incarvito,[†] Michael Bühl,[§] and John F. Hartwig*,[†]

Contribution from the Department of Chemistry, Yale University, P.O. Box 208107, New Haven, Connecticut 06520-8107, and Max-Planck-Institut für Kohlenforschung, Kaiser-Wilhelm-Platz 1, D-45470 Mülheim an der Ruhr, Germany

Received August 14, 2003; E-mail: john.hartwig@yale.edu

Abstract: A series of monomeric arylpalladium(II) complexes LPd(Ph)X (L = 1-AdP^{t}Bu$_2$, P^{t}Bu$_3$, or Ph$_5$FcP^{t}Bu$_2$ (Q-phos); X = Br, I, OTf) containing a single phosphine ligand have been prepared. Oxidative addition of aryl bromide or aryl iodide to bis-ligated palladium(0) complexes of bulky, trialkylphosphines or to Pd(dba)$_2$ (dba = dibenzylidene acetone) in the presence of 1 equiv of phosphine produced the corresponding arylpalladium(II) complexes in good yields. In contrast, oxidative addition of phenyl chloride to the bis-ligated palladium(0) complexes did not produce arylpalladium(II) complexes. The oxidative addition of phenyl triflate to PdL$_2$ (L = 1-AdP^{t}Bu$_2$, P^{t}Bu$_3$, or Q-phos) also did not form arylpalladium(II) complexes. The reaction of silver triflate with (1-AdP^{t}Bu$_2$)Pd(Ph)Br furnished the corresponding arylpalladium(II) triflate in good yield. The oxidative addition of phenyl bromide and iodide to Pd(Q-phos)$_2$ was faster than oxidative addition to Pd(1-AdP^{t}Bu$_2$)$_2$ or Pd(P^{t}Bu$_3$)$_2$. Several of the arylpalladium complexes were characterized by X-ray diffraction. All of the arylpalladium(II) complexes are T-shaped monomers. The phenyl ligand, which has the largest trans influence, is located trans to the open coordination site. The complexes appear to be stabilized by a weak agostic interaction of the metal with a ligand C−H bond positioned at the fourth-coordination site of the palladium center. The strength of the Pd···H bond, as assessed by tools of density functional theory, depended upon the donating properties of the ancillary ligands on palladium.

Introduction

A vacant coordination site on a transition-metal complex is required for many classic organometallic reactions.[1,2] Therefore, unsaturated metal complexes are proposed as intermediates in most metal-catalyzed reactions, such as hydrogenation,[3] hydroformylation,[4,5] olefin polymerization,[6,7] and palladium-catalyzed cross-coupling reactions.[8−11] Many of the palladium-catalyzed cross-couplings are proposed to proceed through unsaturated, three-coordinate arylpalladium(II) halide complexes (Figure 1).

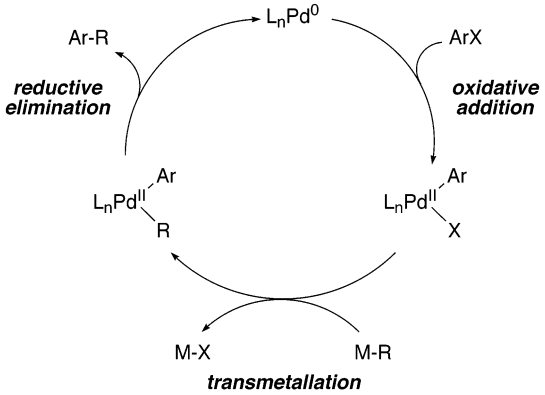

Figure 1. Proposed catalytic cycle for many cross-coupling reactions.

Such intermediates are believed to form directly from oxidative addition of an aryl halide to a zerovalent palladium source with a bulky ligand[12−14] or by dissociation of a dative ligand from a four-coordinate arylpalladium halide complex prior to transmetalation[15] and reductive elimination.[16]

[†] Yale University.
[§] Max-Planck-Institut für Kohlenforschung.

(1) Crabtree, R. H. *The Organometallic Chemistry of the Transition Metals*, 3rd ed.; John Wiley & Sons: New York, 2001.
(2) Collman, J. P.; Hegedus, L. S.; Norton, J. R.; Finke, R. G. *Principles and Applications of Organotransition Metal Chemistry*; University Science Books: Mill Valley, 1987.
(3) Halpern, J. *Inorg. Chim. Acta* **1981**, *50*, 11.
(4) Casey, C. P.; Whiteker, G. T.; Melville, M. G.; Petrovich, L. M.; Gavney, J. A., Jr.; Powell, D. R. *J. Am. Chem. Soc.* **1992**, *114*, 5535.
(5) Breit, B.; Winde, R.; Mackewitz, T.; Paciello, R.; Harms, K. *Chem.−Eur. J.* **2001**, *7*, 3106.
(6) Shultz, L. H.; Tempel, D. J.; Brookhart, M. *J. Am. Chem. Soc.* **2001**, *123*, 11539.
(7) Liu, Z. X.; Somsook, E.; White, C. B.; Rosaaen, K. A.; Landis, C. R. *J. Am. Chem. Soc.* **2001**, *123*, 11193.
(8) Culkin, D. A.; Hartwig, J. F. *Acc. Chem. Res.* **2003**, *36*, 234.
(9) Hartwig, J. F. *Pure Appl. Chem.* **1999**, *71*, 1417.
(10) Miyaura, N.; Yanagi, T.; Suzuki, A. *Synth. Commun.* **1981**, *11*, 513.
(11) Milstein, D.; Stille, J. K. *J. Am. Chem. Soc.* **1979**, *101*, 4992.
(12) Stambuli, J. P.; Bühl, M.; Hartwig, J. F. *J. Am Chem. Soc.* **2002**, *124*, 9346.
(13) Hartwig, J. F.; Paul, F. *J. Am. Chem. Soc.* **1995**, *117*, 5373.
(14) Aranyos, A.; Old, D. W.; Kiyomori, A.; Wolfe, J. P.; Sadighi, J. P.; Buchwald, S. L. *J. Am. Chem. Soc.* **1999**, *121*, 4369.

10.1021/ja037928m CCC: $27.50

The observation and isolation of monomeric three-coordinate arylpalladium(II) halide complexes are rare. Several arylpalladium halide complexes containing an aryl group, a halide, and a single phosphine or arsine ligand have been isolated, but these complexes are typically stabilized by coordination of solvent or by dimerization. Amatore and Jutand detected by NMR spectroscopy an arylpalladium(II)iodide complex with a single arsine ligand, but the vacant site of this complex was occupied by a strongly coordinating solvent such as DMF.[17] Arylpalladium(II) halide complexes ligated by a single hindered P(*o*-tol$_3$) have also been isolated, but these complexes are dimeric with bridging halide ligands.[18,19] Evidence for an equilibrium between a biscarbene arylpalladium halide complex and a species generated by dissociation of one carbene was recently reported, but the structure of the complex resulting from ligand dissociation was not determined.[20]

Three-coordinate d^8 complexes of other metals have been isolated. For example, addition of $AgPF_6$ to $(PPh_3)_3RhCl$ generated $(PPh_3)_3Rh^+$,[21] and addition of $LiN(SiMe_3)_2$ to $(PPh_3)_3$-RhCl generated $(PPh_3)_2RhN(SiMe_3)_2$[22] in studies many years ago. More recently, Hofmann has prepared a three-coordinate Rh^I complex that contains a bulky bidentate phosphine and a neopentyl group.[23] This complex is stabilized by an agostic interaction between a γ-C−H bond on the neopentyl group and the Rh^I center.

A method to prepare arylpalladium halide complexes with a single phosphine donor would facilitate fundamental studies on structure and reactivity of a class of compound that serves as a reactive intermediate in a series of catalytic processes that are widely used in synthetic organic chemistry.[24] We recently synthesized the first examples of arylpalladium(II) complexes that are monomeric, possess a single phosphine ligand, and lack coordinated solvent.[12] These complexes were formed by oxidative addition of phenyl bromide or phenyl iodide to a combination of Pd(dba)$_2$ (dba = dibenzylidene acetone) and a hindered trialkylphosphine and by oxidative addition of aryl iodide to PdL$_2$, with L = P^{t}Bu$_3$. Although four compounds with this coordination sphere were isolated, a more general method was needed if a series of these compounds were to be isolated.

Here we describe such improved methods and the use of this method to prepare a series of new three-coordinate arylpalladium halide complexes containing trialkyl and ferrocenyl dialkylphosphines and the conversion of these complexes to arylpalladium triflate complexes that have been inaccessible by oxidative addition. Extensive structural data and computational studies provide a better understanding of the origin of the low-coordinate, mononuclear structures. All of the arylpalladium halide and triflate complexes in this work were isolated as monomeric species with a single phosphine ligand and without coordinated solvent.

Scheme 1

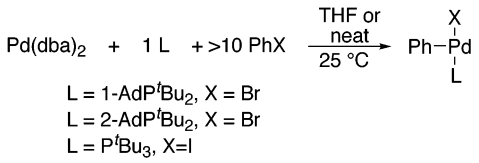

Results

1. Synthesis of LPd(Ar)(Br) and LPd(Ar)(I) by Oxidative Addition. Reaction of the combination of Pd(dba)$_2$ and the hindered alkyl phosphine ligand P^{t}Bu$_3$ or (1-adamantyl)P^{t}Bu$_2$ [(1-Ad)P(^{t}Bu)$_2$] with a large excess of phenyl bromide generated monomeric arylpalladium(II) bromide complexes containing a single phosphine ligand (Scheme 1). However, the presence of dba as a side product complicated the isolation of these low-coordinate palladium complexes. In the presence of dba, the arylpalladium complexes formed the palladium(I) dimer, [1-Ad^t-Bu$_2$PPdBr]$_2$ [25] and 1,1,5-triphenylpenta-1,4-dien-3-one (eq 1). The organic product most likely was formed by the insertion of dba into the Pd−C bond of the arylpalladium(II) halide followed by β-hydride elimination, as would occur in a Heck reaction,[26] and the palladium product was most likely formed by decomposition of the hydrido halide complex to form the stable palladium(I) dimer.[27] Thus, a more general procedure for generating these complexes with a variety of aryl halides and ligands was needed.

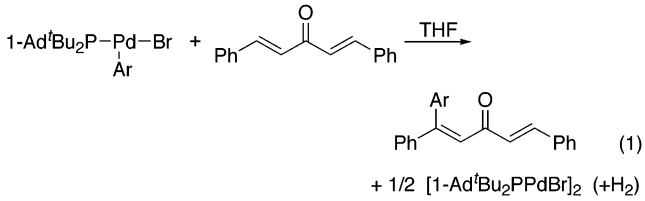

1.1 Development of a Method To Prepare LPd(Ar)(X) L = 1-AdP^{t}Bu$_2$, P^{t}Bu$_3$. Reactions of PdL$_2$ (L = (1-Ad)P^{t}Bu$_2$ **1a** or P^{t}Bu$_3$ **1b**) with aryl halides in THF solvents would eliminate the presence of dba and its complicating side reactions. However, the oxidative addition of aryl halides to these palladium(0) complexes are not favorable thermodynamically in dilute solutions, and reactions of aryl halides with **1a** and **1b** in THF solvent required elevated temperatures (70 °C) and long reaction times (>16 h for phenyl bromide), even when a 40-fold excess of aryl halide was used. The long reaction times led to formation of side products including L$_2$Pd(H)Br[12,28] and [HPR$_3$]$_2$[PdBr$_4$].[29] The presence of these species prevented isolation of pure arylpalladium(II) halide complexes by this method.

A high concentration of phenyl bromide could cause the oxidative addition products to form from the palladium(0) species in higher conversions and with faster rates without influencing the rate of decomposition of the arylpalladium halide

(15) Ricci, A.; Angelucci, F.; Bassetti, M.; Lo Sterzo, C. *J. Am. Chem. Soc.* **2002**, 1060.
(16) Ozawa, F.; Ito, T.; Nakamura, Y.; Yamamoto, A. *Bull. Chem. Soc. Jpn.* **1981**, *54*, 1868.
(17) Amatore, C.; Bahsoun, A. A.; Jutand, A.; Meyer, G.; Ntepe, A. N.; Ricard, L. *J. Am. Chem. Soc.* **2003**, *125*, 4212.
(18) Paul, F.; Patt, J.; Hartwig, J. F. *Organometallics* **1995**, *14*, 3030.
(19) Widenhoefer, R. A.; Zhong, H. A.; Buchwald, S. L. *Organometallics* **1996**, *15*, 2745.
(20) Lewis, A. K. d. K.; Caddick, S.; Cloke, F. G. N.; Billingham, N. C.; Hitchcock, P. B.; Leonard, J. *J. Am. Chem. Soc.* **2003**, *125*, 10066.
(21) Uma, R.; Davies, M. K.; Crévisy, C.; Grée, R. *Eur. J. Org. Chem.* **2001**, 3141.
(22) Cetinkaya, B.; Lappert, M. F.; Torroni, S. *J. Chem. Soc., Chem. Commun.* **1979**, 843.
(23) Urtel, H.; Meier, C.; Eisentrager, F.; Rominger, F.; Joschek, J. P.; Hofmann, P. *Angew. Chem., Int. Ed.* **2001**, *40*, 781.
(24) Hegedus, L. S. *Transition Metals in the Synthesis of Complex Organic Molecules*, 2nd ed.; University Science Books: Sausalito, CA, 1999.
(25) Stambuli, J. P.; Kuwano, R.; Hartwig, J. F. *Angew. Chem., Int. Ed.* **2002**, *41*, 4746.
(26) Amatore, C.; Jutand, A. *Acc. Chem. Res.* **2000**, *33*, 314.
(27) Dura-Vila, V.; Mingos, D. M. P.; Vilar, R.; White, A. J. P.; Williams, D. J. *J. Organomet. Chem.* **2000**, *600*, 198.
(28) Clark, H. C.; Goel, A. B.; Goel, S. *J. Organomet. Chem.* **1979**, *166*, C29.
(29) Goel, R. G.; Montemayor, R. G. *Inorg. Chem.* **1977**, *16*, 2183.

Scheme 2

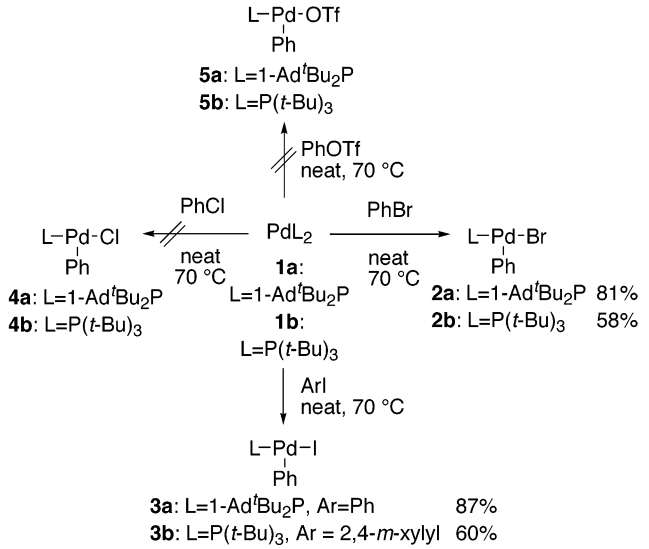

complexes. Thus, the reactions of PdL_2 [L = 1-AdP^tBu_2(**1a**), P^tBu_3(**1b**)] were evaluated in neat aryl bromide.

1.2. Preparation of LPd(Ar)(X), L = 1-AdP^tBu_2, P(^{t}Bu)$_3$. Scheme 2 summarizes the oxidative addition reactions that form T-shaped arylpalladium bromide and iodide complexes ligated by 1-AdP^tBu_2 and P(^{t}Bu)$_3$. Warming of 1-adamantyl di-*tert*-butylphosphine and tri-*tert*-butylphosphine palladium(0) complexes **1a**,**b** in neat phenyl bromide and phenyl iodide formed the oxidative addition products **2a**,**b** and **3a**,**b** at 70 °C. The adamantylphosphine-ligated bromide and iodide complexes **2a** and **3a** were isolated in high yields after addition of pentane to the aryl halide solution, but the tri-*tert*-butylphosphine complexes **2b** and **3b** were isolated in somewhat lower yields.

The oxidative addition of phenyl chloride generally occurs more slowly than the addition of phenyl bromide and iodide,[30] but Pd(0) complexes of P^tBu_3 and 1-AdP^tBu_2 catalyze the coupling of aryl chlorides under mild conditions.[25,31] Despite this catalytic activity of P^tBu_3 and 1-AdP^tBu_2 palladium complexes, no arylpalladium(II) chloride complexes were observed by ^{31}P NMR spectroscopy after heating of Pd(0) complexes **1a** or **1b** in neat phenyl chloride at 70 °C for 20 h. Only the starting palladium(0) complex and free ligand were observed by ^{31}P NMR spectroscopy. We have previously established an equilibrium between the combination of free chlorotoluene and [Pd(P^tBu_3)$_2$] and the combination of the arylpalladium chloride complex and free P^tBu_3. This solution contains smaller amounts of the arylpalladium chloride complex than the Pd(0) complex, even in neat chlorotoluene.[32] Thus, oxidative addition of chloroarenes to these Pd(0) complexes cannot generate high yields of arylpalladium chloride complexes containing unactivated aryl groups for thermodynamic reasons, and the inability to observe the phenylpalladium chloride complex is likely due to the instability of the product over long times at elevated temperatures.

The addition of phenyl triflate often occurs at rates similar to those for the addition of phenyl bromide.[33] However, few catalytic couplings of aryl triflates catalyzed by complexes of

(30) Grushin, V. V.; Alper, H. *Chem. Rev.* **1994**, *94*, 1047.
(31) Littke, A. F.; Fu, G. C. *J. Am. Chem. Soc.* **2001**, *123*, 6989.
(32) Roy, A. H.; Hartwig, J. F. *J. Am. Chem. Soc.* **2001**, *123*, 1232.
(33) Jutand, A.; Mosleh, A. *Organometallics* **1995**, *14*, 1810.

Scheme 3

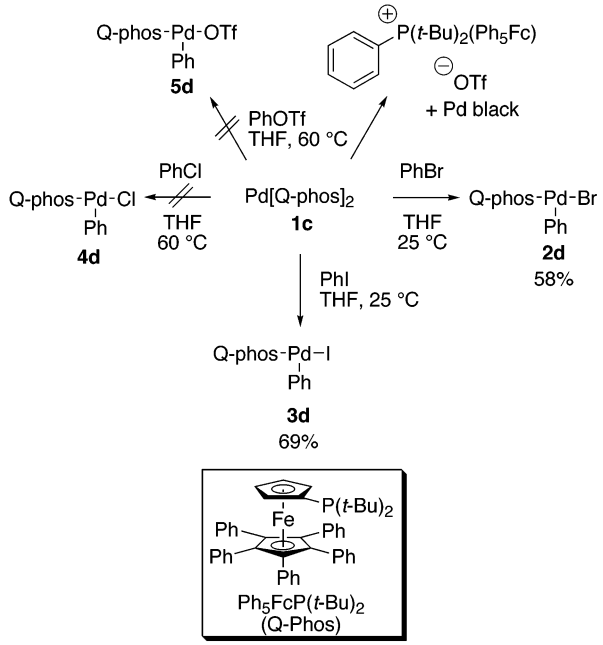

P(^{t}Bu)$_3$ or 1-AdP^tBu_2 have been reported.[34] The reactions of **1a** and **1b** with phenyl triflate at 70 °C produced several products, none of which displayed NMR signals consistent with the arylpalladium triflate complex **5a**.

1.3. Preparation of LPd(Ar)(X) Complexes with Related Hindered Phosphines. 1.3.1. L = 2-AdP^tBu_2. The reaction conditions of neat aryl halide required for the formation of **2a**,**b** in high yield were not necessary to generate the arylpalladium(II) bromide complex (2-Ad^{t}Bu$_2$P)Pd(Br)Ph (**2c**) containing the less hindered 2-adamantyl-di-*tert*-butylphosphine ligand (2-AdP^tBu_2). Reaction of Pd(dba)$_2$, 1 equiv of 2-AdP^tBu_2, and 40 equiv of PhBr in THF solvent at 25 °C formed the oxidative addition product **2c** in 86% yield after addition of pentane to the reaction solution (eq 2). Pd(dba)$_2$ was a suitable precursor because complex **2c** was more stable toward dba and less soluble than complexes **2a**,**b** with more hindered trialkylphosphines.

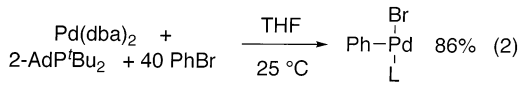

1.3.2. L = 1-di-*tert*-butylphosphino-1′,2′,3′,4′,5′-pentaphenylferrocene (Q-phos). Reactions of the Pd(0) complex ligated by 1-di-*tert*-butylphosphino-1′,2′,3′,4′,5′-pentaphenylferrocene (Q-phos) with aryl halides and triflates are summarized in Scheme 3. Reaction of (Q-phos)$_2$Pd(0) with phenyl bromide and iodide occurred in THF to form the arylpalladium halide complexes **2d** and **3d** with a single phosphine ligand in 58 and 69% isolated yield, respectively. These reactions occurred at room temperature instead of at 70 °C, as required for reactions of **1a**,**b**. Again, treatment of the palladium(0) complex with phenyl chloride did not produce an oxidative addition product. Only free Q-phos and starting **1c** were detected by ^{31}P NMR spectroscopy after heating of **1c** for 20 h at 60 °C in phenyl chloride. Free ligand and palladium metal were observed at higher temperatures.

(34) Littke, A.; Dai, C.; Fu, G. *J. Am. Chem. Soc.* **2000**, *122*, 4020.

Scheme 4

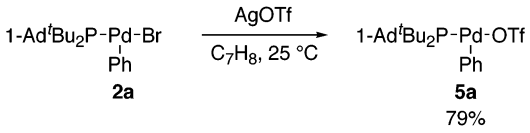

Reaction of phenyl triflate with complex **1c** at 60 °C for 2 h produced the arylphosphonium salt of Q-phos, $[FcP(Ph)^tBu_2(Ph)_5]^+[OTf]^-$. The same phosphonium salt was also generated by the addition of silver triflate to a solution of the Q-phos-ligated bromide complex **2d**. No reaction occurred between free Q-phos and the aryl triflate at 60 °C over the same time frame, which implies that the P−C bond is formed at the metal center. Most likely, the arylpalladium triflate complex is unstable to P−C bond-forming reductive elimination of the phosphonium salt.

2. Independent Route to LPd(Ph)(OTf) (L = (1-Ad)P(^{t}Bu)$_2$). A route to the arylpalladium triflate complex ligated by (1-Ad)P(^{t}Bu)$_2$ was developed starting from the phenylpalladium bromide complex, as shown in Scheme 4. Treatment of bromide complex **2a** with silver triflate in toluene at room temperature produced palladium triflate **5a** in good yield. Complex **5a** decomposed to many products when heated at 70 °C for 2 h, and this thermal instability explains the difficulty in isolating this complex from an oxidative addition at this temperature. The infrared spectrum of triflate **5a** in THF solution showed that the triflate was coordinated to palladium. Free triflate typically vibrates at 1280 cm^{-1}, and coordinated triflates vibrate closer to 1380 cm^{-1}.[35] The infrared spectrum of **5a** in solution contained a band at 1395 cm^{-1}. Moreover, the ^{31}P NMR chemical shift in the relatively nonpolar noncoordinating solvent benzene was similar to that in THF. The infrared spectrum of **5a** as a KBr pellet in the solid state was less conclusive. This spectrum contained a strong band at 1317 cm^{-1}, which falls between the typical frequencies for free and bound triflates. X-ray crystallography, however, showed that the triflate was bound to palladium in the solid state as well (vide infra).

3. Spectroscopic Characteristics. All of the arylpalladium halide and triflate complexes were fully characterized by common spectroscopic techniques; all but one complex were amenable to microanalysis. Several complexes were characterized by X-ray diffraction, as described below. The 1:1 ratio of phosphine to palladium in each of the isolated complexes was determined by integration of the resonances of the phosphine versus those of the palladium-bound aryl group. One might expect that the ^{31}P NMR chemical shifts of the complexes in this work would differ from those of phosphine ligands in more conventional coordination spheres. However, no clear trends in chemical shifts could be gleaned from comparisons of the shifts of the three-coordinate palladium(II) relative to those of dimeric arylpalladium halide complexes, bisphosphine arylpalladium halide complexes, or the respective palladium(0) precursors. The mononuclearity of these complexes was determined by X-ray diffraction.

3.1. Evaluation of Potential Agostic Interactions by ^{1}H and ^{13}C NMR and IR Spectroscopic Studies. We probed for the presence of an agostic interaction in each complex by infrared and low-temperature ^{1}H NMR and ^{13}C NMR spectroscopy. The infrared spectra of many agostic compounds contain a medium-strong infrared band at frequencies lower than those of typical C−H stretches. The ^{1}H NMR chemical shift of the hydrogen involved in a C−H agostic interaction is typically shifted upfield from its position when unbound to the metal, and the C−H coupling constant involving an agostic hydrogen is often lower than that of the analogous free C−H bond.[36,37]

All infrared spectra of the P(^{t}Bu)$_3$, (1-Ad)P(^{t}Bu)$_2$, and Q-phos complexes showed that any agostic interaction must be weak. The infrared spectra of free ligands 1-AdP^{t}Bu$_2$, P^{t}Bu$_3$, and Q-phos contained C−H bands between 3000 and 2800 cm^{-1}. The infrared spectra of **2a**−**5a**, **2b**−**3b**, and **2d**−**3d** did not contain any medium-strong C−H stretching bands below 2800 cm^{-1} that would indicate a weakened C−H bond resulting from an agostic interaction.

In contrast, the infrared spectrum of complex **2c** containing the 2-adamantyl ligand contained a weakened C−H stretching band that clearly indicates the presence of an agostic interaction. The infrared spectrum of free 2-AdP^{t}Bu$_2$ contained C−H bands from 3000 to 2850 cm^{-1}. The infrared spectrum of complex **2c** contained a medium-strong band at 2700 cm^{-1}. Thus, the agostic interaction in complex **2c** with the secondary carbon attached to phosphorus appears to be stronger than that in the complexes with the larger ligands. This stronger agostic interaction and the increased rigidity of the ligand that would result from this interaction may account for some of the increased stability and lower solubility of this complex, relative to those of the arylpalladium halides with the larger 1-AdP^{t}Bu$_2$ and P^{t}Bu$_3$ ligands.

None of the ^{1}H or ^{13}C NMR spectra of the arylpalladium complexes in this work provided evidence for an agostic interaction. ^{1}H NMR spectra of complexes **2b**, **2d**, and **3d** were obtained from room temperature to −100 °C in CD_2Cl_2, and ^{1}H NMR spectra of (1-Ad)P(^{t}Bu)$_2$ complex **2a**, and (2-Ad)P(^{t}Bu)$_2$ complex **2c** were obtained between 20 °C and −115 °C in $CDCl_2F$.[38] The ^{1}H NMR spectra of Q-phos-ligated complexes **2d** and **3d** broadened at low temperatures because of conformational changes of the pentaphenylferrocenyl group on the NMR time scale, but no resonance emerged at high field at −90 °C in CD_2Cl_2. The ^{1}H NMR spectrum of (2-Ad)P(^{t}Bu)$_2$ complex **2c** in $CDCl_2F$ at −115 °C was complex due to its low symmetry, and it was also broadened at this temperature. However, no upfield resonance that would signify an agostic interaction was observed at this low temperature. In addition, we measured the C−H coupling constants of the ligand hydrogens by two-dimensional J-resolved ^{13}C NMR spectroscopic methods, and no evidence for a reduced value of these couplings in the complexes was obtained. Even the methine J^1_{CH} values of the 2-adamantyl complex **2c**, which showed reduced C−H stretching frequencies, were within 1.5 Hz of those of the free ligand. The lack of an upfield shift and reduced C−H coupling constant in these complexes could result from the absence of an agostic interaction in solution, a small upfield shift and change in coupling constant from the agostic interaction, or a small change in value and an equilibration of the agostic and free hydrogens at a rate faster than the NMR time scale. Computational studies described in section 4 imply that there is a small difference in chemical shift between the agostic and free hydrogens.

(35) Lawrance, G. A. *Chem. Rev.* **1986**, *86*, 17.
(36) Brookhart, M.; Green, M. L. H.; Wong, L. L. *Prog. Inorg. Chem.* **1988**, *36*, 1.
(37) Brookhart, M.; Green, M. L. H. *J. Organomet. Chem.* **1983**, *250*, 395.
(38) Siegel, J. S.; Anet, F. A. L. *J. Org. Chem.* **1988**, *53*, 2629.

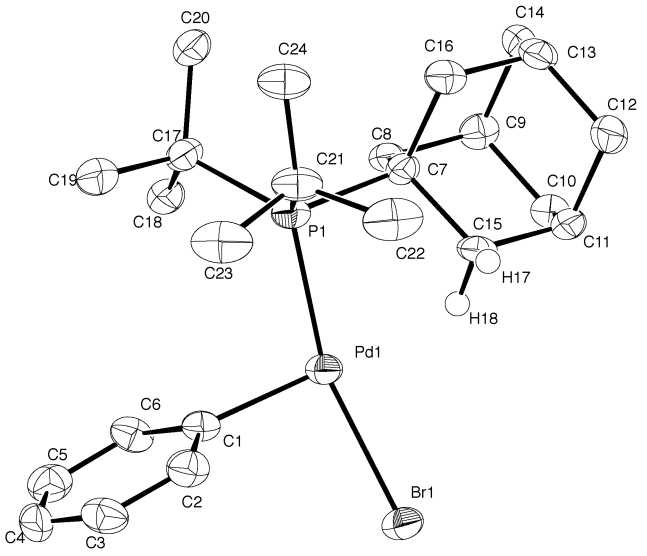

Figure 2. ORTEP diagram of (1-AdP^{t}Bu$_2$)Pd(Ph)Br (**2a**) at 30% ellipsoids.

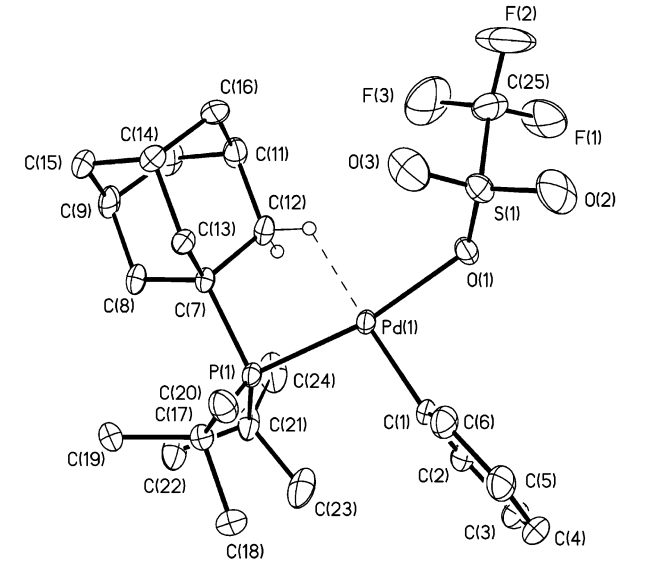

Figure 3. ORTEP diagram of (1-AdP^{t}Bu$_2$)Pd(Ph)OTF (**5a**) at 30% ellipsoids.

3.2. X-ray Diffraction Studies. Several of the arylpalladium halide and triflate complexes were characterized by X-ray diffraction. The ORTEP diagrams of **2a**, **5a**, **2b**, **3b**, and **2d** are pictured sequentially in Figures 2−6. Selected bond angles and distances are presented in Tables 2−4. Each complex adopted a T-shaped geometry with the phenyl group located trans to the open coordination site. Each complex also contained a hydrogen atom of a phosphine ligand located within 2.4 Å of the metal center at the coordination site that lacks a heavy atom. The hydrogen atom nearest the metal in complex **2a** was located and refined. In the other cases, the M−H distances were estimated by placing the hydrogen atoms in idealized positions. The M−H distance depended on the electronic properties of the ancillary ligands in a fashion that could be rationalized by considering the electrophilicity of the metal. The more electrophilic the metal center, the shorter the M−H distance. Therefore, the metal coordination sphere of these complexes contains three conventional metal−ligand bonds and an additional weak agostic interaction together in a square-planar arrangement.

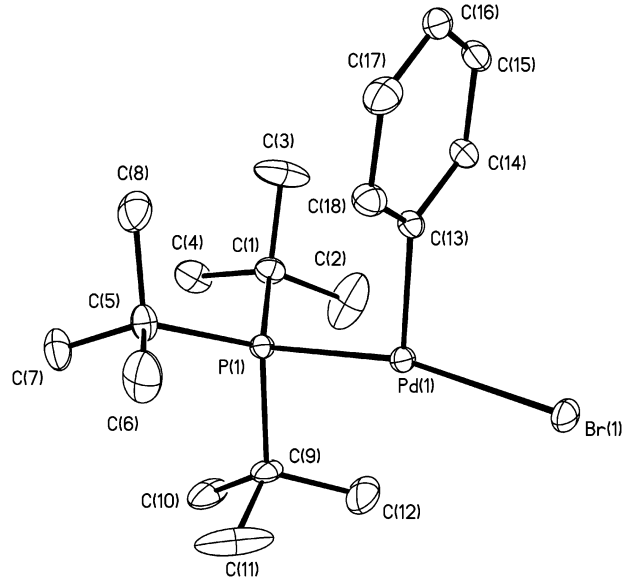

Figure 4. ORTEP diagram of P(^{t}Bu)$_3$Pd(Ph)Br (**2b**) at 30% ellipsoids.

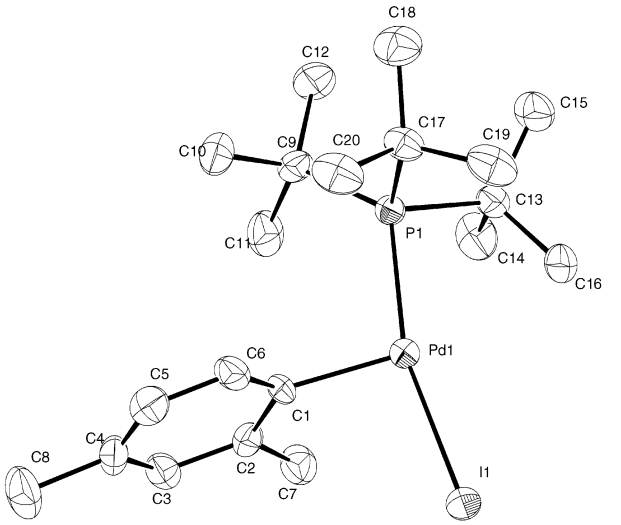

Figure 5. ORTEP diagram of P^{t}Bu$_3$Pd(*m*-xylyl)I (**3b**) at 30% ellipsoids.

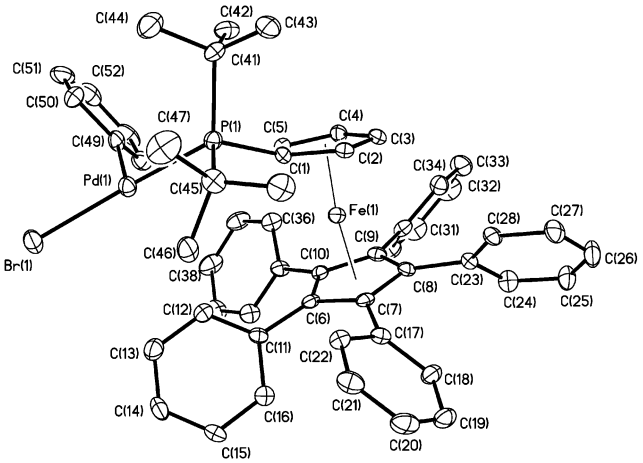

Figure 6. ORTEP diagram of (Q-phos)Pd(Ph)Br (**2d**) at 30% ellipsoids.

As seen in Table 1, the Pd−P and Pd−C$_{ipso}$ bond distances were similar among all the compounds. Complex **5a** has the shortest Pd−P bond distance, which may be a result of the weak

Table 1. Bond Distances (in angstroms) of Arylpalladium(II) Halide Complexes Determined by X-ray Diffraction and Values Determined from DFT (BP86/ECP1 level, in parentheses)

complex	Pd–P	Pd–C	Pd–X	Pd···H[a]	Pd···C[a]
2a, L = 1-AdP^{t}Bu$_2$, X = Br	2.296(1)	1.977(4)	2.4711(5)	2.26(3)	2.799(4)
	(2.331)	(1.989)	(2.444)	(2.284)	(3.012)
2c, L = 2-AdP^{t}Bu$_2$, X = Br	nd[b]	nd	nd	nd	nd
	(2.319)	(1.998)	(2.451)	(2.154)	(3.155)
5a, L = 1-AdP^{t}Bu$_2$, X = OTf	2.2523(16)	1.967(3)	2.159(2)	2.06[c]	2.74[c]
	(2.320)	(1.979)	(2.221/2.348)	(2.730)	(3.426)
2b, L = P^{t}Bu$_3$, X = Br	2.2854(13)	1.977(5)	2.4537(8)	2.18[c]	2.81[c]
	(2.332)	(1.987)	(2.438)	(2.421)	(3.087)
3b (3b′),[a] L = P^{t}Bu$_3$, X = I	2.294(1)	1.982(4)	2.6126(4)	2.33[c]	2.94[c]
	(2.347)	(1.989)	(2.620)	(2.461)	(3.142)
2d, L = Q-phos, X = Br	2.2567(10)	1.969(3)	2.4292(6)	2.13[c]	2.78[c]

[a] Experiment for **3b** with Ar = 2,4-*m*-xylyl; DFT results for **3b′** with Ar = Ph. [b] Not determined. [c] Determined from idealized positions.

Table 2. Bond Angles (in degrees) of Arylpalladium(II) Halide Complexes Determined by X-ray Diffraction and Values Determined by DFT (BP86/ECP1 level, in parentheses)

complex	P–Pd–C	X–Pd–C	X–Pd–P
2a, L = 1-AdP^{t}Bu$_2$, X = Br	100.8(1)	91.4(1)	162.61(3)
	(102.9)	(92.8)	(164.2)
2c, L = 2AdP^{t}Bu$_2$, X = Br	(98.8)	(92.0)	(169.2)
5a, L = 1-AdP^{t}Bu$_2$, X = OTf	100.58(9)	90.29(10)	169.12(5)
	(99)	(88)	(171)
2b, L = P^{t}Bu$_3$, X = Br	99.92(15)	93.14(5)	166.88(4)
	(103.0)	(93.9)	(163.0)
3b(3b′),[a] L = P^{t}Bu$_3$, X = I	100.9(1)	94.0(1)	164.57(3)
	(102.6)	(94.6)	(162.4)
2d, L = Q-phos, X = Br	100.71(11)	91.94(11)	166.16(3)

[a] Experiment for **3b** with Ar = 2,4-*m*-xylyl; DFT results for **3b′** with Ar = Ph.

electron-donating ability of the triflate ligand bound to palladium. The Pd−O bond length in triflate **5a** is shorter than the palladium−halogen bond lengths because of the smaller size of the oxygen atom. The palladium−bromide bond distances did not vary with changes in the phosphine ligand.

The bond angles of the coordination sphere of the metal are shown in Table 2. All of the complexes that were examined by X-ray analysis have angles about the palladium that total approximately 360°, but the angles deviated significantly from 90 or 180°. The P−Pd−C$_{ipso}$ bond angles are all about 10° larger than the idealized 90° angle of a T-shaped geometry. In contrast, the X−Pd−C$_{ipso}$ and X−Pd−P bond angles varied significantly between complexes of the different ligands. For instance, P^{t}Bu$_3$-ligated **2b** and **3b** have X−Pd−C$_{ipso}$ angles greater than 93°, while the 1-AdP(^{t}Bu)$_2$- and Q-phos-ligated complexes **2a** and **2d** have X−Pd−C$_{ipso}$ angles less than 92°. The magnitudes of the X−Pd−P bond angles were found to vary with the identity of the halide. Bromide complexes **2b** and **2d** contain X−Pd−P angles around 166°, while the triflate complex **5a** has a larger angle of 169° and the iodide **3b** has a smaller angle of 165°. The 1-adamantyl-ligated bromide complex **2a** has an X−Pd−P angle of 163°, which is much different from the same angle in bromides **2b** and **3b** and is the smallest X−Pd−P angle of the complexes we studied.

The overall conformation and detailed metrical parameters of the phosphine ligand provide information on how the complexes accommodate their steric bulk. The adamantyl cages of the phosphines in complexes **2a** and **5a** are positioned nearest to the open coordination site. In contrast, the largest group on the Q-phos ligand, the pentaphenylcyclopentadienyl group, is positioned distal to the open coordination site in **2d**. Thus, the substituent that occupies the largest volume of the ligand appears to occupy the open coordination site if this substituent can donate a hydrogen atom to the metal. One might expect an aryl group of the pentaphenylferrocenyl unit to bind to the open site, but these groups are located further from the metal than the nearest hydrogen of the *tert*-butyl group and in an inappropriate geometry to donate to the metal.

Distortions in bond angles at phosphorus are revealed by the angles summarized in Table 3. The phosphine ligands in all the complexes pivot at the phosphorus toward the open coordination site. The Pd−P−C angle that includes the alkyl group nearest the metal was found to be 12−24° smaller than the next smallest of the Pd−P−C angles. Moreover, the P−C−C angle that includes the carbon bearing the hydrogen closest to the metal was smaller than the other two P−C−C angles. This difference in P−C−C angles was smaller than the difference in Pd−P−C angles but was statistically significant. The P−C−C angle that includes the carbon bearing the hydrogen nearest the metal was found to be 1.2−6.6° smaller than the next smallest of the other two P−C−C angles. The P−Pd−C bond angle was found to be smaller in the complexes that contain the smaller Pd···H distance. The triflate complex **5a**, which has the shortest Pd···H distance of 2.06 Å, has the smallest P−Pd−C bond angle of 92.31(9)°, while complex **3b**, which has the largest Pd···H bond distance of 2.33 Å, has the largest P−Pd−C bond angle of 96.5(1)°. These distortions are consistent with the presence of an agostic interaction that would require a distortion of the angles at phosphorus and at the *tert*-butyl or adamantyl carbon bound to phosphorus, but they may also simply originate from a drive to relieve steric congestion. For example, Caulton and co-workers reported that the one P−Ru−C bond angle in RuCl$_2$(CO)(P^{i}Pr$_3$)$_2$ was 10° smaller than the smaller of the other two P−Ru−C angles,[39] but the Ru···H distance of this complex was longer than would be characteristic of an agostic interaction. Likewise, one Pd−P−C angle of the tri-*o*-tolylphosphine ligand in {Pd[P(*o*-tol)$_3$](*p*-C$_6$H$_4$-*n*-Bu)Br}$_2$ was found to be 5° smaller than the smaller of the other two angles, and this complex contains square-planar coordination geometries with no agostic interactions.[18]

4. Computational Studies of 2a, 2b, 3b′, and 2c. To complement the experimental studies and to provide a further assessment of the presence or absence of an agostic bonding interaction, computational studies were conducted. Several complexes, including those prepared recently[40] and some

(39) Huang, D.; Streib, W. E.; Bollinger, J. C.; Caulton, K. G.; Winter, R. F.; Scheiring, T. *J. Am. Chem. Soc.* **1999**, *121*, 8087.
(40) Gerisch, M.; Krumper, J. R.; Bergman, R. G.; Tilley, T. D. *Organometallics* **2003**, *22*, 47.

Table 3. Bond Angles Containing the Phosphorus Atom of Complexes **2a**, **5a**, **2b**, and **3b** Determined by X-ray Diffraction

complex	atoms	angle (deg)	atoms	angle (deg)
2a	Pd(1)−P(1)−C(7)	95.5(1)	P(1)−C(7)−C(15)	106.0(3)
L = 1-AdP^{t}Bu$_2$, X = Br	Pd(1)−P(1)−C(21)	109.0(1)	P(1)−C(7)−C(8)	110.9(3)
	Pd(1)−P(1)−C(17)	122.7(1)	P(1)−C(7)−C(16)	116.9(3)
5a	Pd(1)−P(1)−C(7)	92.31(9)	P(1)−C(7)−C(12)	105.83(16)
L = 1-AdP^{t}Bu$_2$, X = OTf	Pd(1)−P(1)−C(21)	113.99(9)	P(1)−C(7)−C(13)	110.52(14)
	Pd(1)−P(1)−C(17)	118.60(8)	P(1)−C(7)−C(8)	116.48(17)
2b	Pd(1)−P(1)−C(9)	93.79(19)	P(1)−C(9)−C(12)	106.6(5)
L = P^{t}Bu$_3$, X = Br	Pd(1)−P(1)−C(1)	115.0(19)	P(1)−C(9)−C(11)	107.8(6)
	Pd(1)−P(1)−C(5)	116.9(2)	P(1)−C(9)−C(10)	118.1(5)
3b	Pd(1)−P(1)−C(13)	96.5(1)	P(1)−C(13)−C(16)	107.9(3)
L = P^{t}Bu$_3$, X = I	Pd(1)−P(1)−C(17)	108.2(1)	P(1)−C(13)−C(14)	109.7(3)
	Pd(1)−P(1)−C(9)	123.0(1)	P(1)−C(13)−C(15)	117.0(3)
2d	Pd(1)−P(1)−C(45)	94.52(12)	P(1)−C(45)−C(46)	104.0(2)
L = Q-phos, X = Br	Pd(1)−P(1)−C(1)	118.68(11)	P(1)−C(45)−C(47)	110.6(3)
	Pd(1)−P(1)−C(45)	119.57(12)	P(1)−C(45)−C(48)	117.2(3)

Table 4. Computational Analysis of the Pd···H Interaction in Arylpalladium(II) Halides at the BP86/ECP1 Level (except where otherwise noted)

complex	$\nu_{C-H\cdots Pd}$ cm^{-1}	δ (^{1}H) (ppm)[a]	WBI	ρ (au)	$\nabla\rho$ (au)
2a, L = 1-AdP^{t}Bu$_2$, X = Br	2812	0.6	0.023	0.023	0.075
2c, L = 2-AdP^{t}Bu$_2$, X = Br	2748	−0.4	0.041	0.029	0.083
2b, L = P^{t}Bu$_3$, X = Br	2910	1.1	0.016	0.018	0.058
3b′, L = P^{t}Bu$_3$, X = I	2919	1.3	0.015	0.017	0.053

[a] B3LYP/II″ level.

prepared many years ago,[41] have been termed agostic without ^{1}H NMR or IR spectroscopic evidence.[42−47] Thus, we computed geometries and harmonic vibrational frequencies for several of the complexes and conducted a topological analysis of the total electron density as developed by Bader and termed the atoms-in-molecules (AIM) theory.[48]

Geometries and harmonic vibrational frequencies were computed at the BP86/ECP1 level[49] for complexes **2a** (1-AdP^{t}Bu$_2$-Pd(Ph)Br), **2b** (P^{t}Bu$_3$Pd(Ph)Br), the phenyl analogue of **3b** (P^{t}Bu$_3$Pd(Ph)I, **3b′**), and **2c** (2-AdP^{t}Bu$_2$Pd(Ph)Br). The computed geometrical parameters of **2a**, **2b**, and **3b′** agree well with those determined in the solid state by X-ray diffraction, except for the nonbonded Pd···C distances, which are noticeably overestimated (see Tables 2 and 3). A prime indicator for the presence of an agostic Pd···H interaction is the distance between the palladium and nearest hydrogen atom. The experimental Pd···H bond distance of 2.26 Å for **2a** is close to the optimized value of 2.28 Å (Table 1). The Pd···H distances for P^{t}Bu$_3$-ligated iodide **3b′** and 2-AdP^{t}Bu$_2$-ligated **2c** were computed to be somewhat longer and shorter, respectively, than that in **2a** (2.46 Å and 2.15 Å, Table 1).

Additional computational data providing evidence for a weak agostic interaction are collected in Table 4. Frequency calculations predicted that the C−H vibration involving the hydrogen atom closest to Pd would occur near 2900 cm^{-1} for **2b** and **3b′**, near 2810 cm^{-1} for **2a**, and near 2750 cm^{-1} for **2c**.[50] As predicted by these calculations, the experimental infrared spectrum of **2c** contained a C−H stretch at 2710 cm^{-1}, which is sufficiently far from the standard frequency of C−H stretches to assign it to an agostic interaction.

Calculations of the ^{1}H NMR spectra of **2a**−**c** and **3b′** were also performed. These calculations showed that the static ^{1}H NMR spectrum would show only small differences in chemical shift between the hydrogen located nearest the metal center and the hydrogens distal from the metal in the *tert*-butyl or adamantyl groups. ^{1}H NMR chemical shifts for the agostic hydrogen in the static structures of **2a** and **2c** were calculated to lie near +0.6 ppm and −0.4 ppm, respectively (Table 4). Exchange between the agostic hydrogen and the large number of free *tert*-butyl hydrogens or the appropriate adamantyl hydrogens was fast on the NMR time scale and, therefore, led to averaged chemical shift values that are within the typical range for aliphatic hydrogens. These calculations explain the absence of ^{1}H NMR spectroscopic evidence for metal−hydrogen interactions in **2a** and **2c**.

Population analyses were also used to assess the extent of bonding interactions. The Wiberg bond indices (WBIs)[51] of both P^{t}Bu$_3$ complexes were calculated to be less than 0.02 (Table 4). The WBI of complex **2c**, which appears by experimental data to contain the strongest agostic interaction of the complexes in this work, was 0.04. A yttrium alkyl complex with a hydrogen that appeared by X-ray crystallography to participate in an agostic interaction was computed to have a WBI of 0.013 for its M−H agostic interaction.[42]

Topological analyses of the total electron densities (Bader analyses) were also performed to provide a more precise analysis of the presence or absence of a Pd···H bonding interaction. A bonding interaction between two atoms creates a so-called bond critical point (bcp), which is the saddle point of the electron density between the two nuclei. The magnitude (ρ) of the electron density and its Laplacian(∇_ρ) at the bcp provide information about the strength and type of bond between the two atoms. The ρ value between the two atoms is typically larger for covalent bonds than for ionic and hydrogen bonds and is very small for repulsive interactions. The ∇_ρ is positive for ionic,

(41) Dawoodi, Z.; Green, M. L. H.; Mtetwa, V. S. B.; Prout, K. *Chem. Commun.* **1982**, 802.
(42) Niemeyer, M. *Z. Anorg. Allg. Chem.* **2002**, *628*, 647.
(43) Chen, W.-C.; Hung, C.-H. *Inorg. Chem.* **2001**, *40*, 5070.
(44) Leung, W.-H.; Zheng, H.; Chim, J. L. C.; Chan, J.; Wong, W.-T.; Williams, I. D. *J. Chem. Soc., Dalton Trans.* **2000**, 423.
(45) Pupi, R. M.; Coalter, J. N.; Petersen, J. L. *J. Organomet. Chem.* **1995**, *497*, 17.
(46) Cuenca, T.; Flores, J. C.; Royo, P. *Organometallics* **1992**, *11*, 777.
(47) Bennett, M. A.; Chiraratvatana, C.; Robertson, G. B.; Tooptakong, U. *Organometallics* **1988**, *7*, 1403.
(48) Bader, R. F. W. *Atoms in Molecules*; Oxford Press: New York, 1990.
(49) Jonas, V.; Thiel, W. *J. Chem. Phys.* **1995**, *102*, 8474.
(50) Visual inspection of the corresponding vibrational modes (i.e., eigenvectors) showed that they are clearly localized at the agostic CH bond for **2a** and **2c**, whereas in the case of **2b** and **3b′** some mixing with the other CH stretching modes from the same methyl group was apparent.
(51) Wiberg, K. B. *Tetrahedron* **1968**, *24*, 1083.

Scheme 5

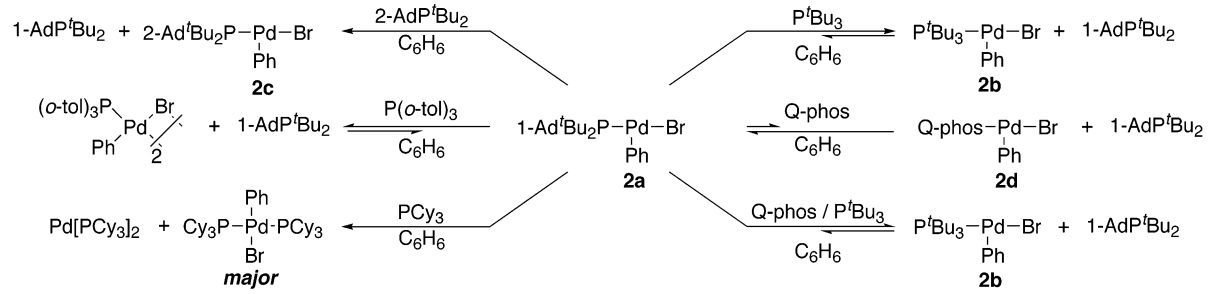

hydrogen, or agostic bonds and negative for covalent bonds. Therefore, the presence of a bcp, a small ρ value, and a positive ∇_ρ value would indicate the presence of an agostic interaction between the palladium and nearest hydrogen of the ligand.

For all complexes **2a**−**c** and **3b′**, a bond path between Pd and the nearest H atom was found and the bcp's showed small values of ρ and small, positive values of $\nabla\rho$. These data indicate that a weak agostic interaction is present in **2a**−**c** and **3b′**. For comparison, calculations of the Pd−H bonding in $Pd(PH_3)_2(H)_2$ showed a WBI of 0.52 and a ρ value of 0.127 au ($\nabla\rho$ = −0.118 au). This comparison suggests that the agostic Pd···H interactions in **2a**,**c** are about 1 order of magnitude weaker than a typical Pd−H single bond. All computational criteria in Tables 2 and 4 indicate that the strength of the Pd···H interaction increases in the sequence **3b′** ≤ **2b** < **2a** < **2c**. Thus, computational studies and IR spectroscopic measurements suggest that complexes **2b** and **3b′** contain weak agostic interactions, while complex **2c** contains a stronger agostic interaction.

The triflate complex **5a** appeared to be a special case for the application of theory to understanding the M···H interaction. In the solid-state structure determined by X-ray diffraction, the triflate was coordinated to palladium in a η^1-fashion, and the adamantyl group was oriented to create a close Pd···H contact (around 2 Å when H atoms are placed at standard positions). When a full geometry optimization was started from this experimental structure, the triflate rotated to place a second oxygen atom near the vacant coordination site and to create an η^2-triflate complex. This coordination in the calculated structure released the agostic hydrogen and created a Pd···H distance of 2.74 Å (Table 1). These computational data do not imply that the complex adopts a structure in the solution phase that is different from that in the solid, but they do suggest that the equilibrium between both coordination modes is finely balanced. If so, the magnitude of the agostic interaction is comparable to the magnitude of the coordination of the second oxygen of a triflate group.

5. Phosphine Ligand Exchange Processes. Ligand substitution reactions of 1-AdP^tBu_2-ligated **2a** were conducted with $P(^tBu)_3$, Q-phos, 2-Ad$P(^tBu)_2$, and several common monodentate phosphines. These reactions are summarized in Scheme 5. The addition of 1 equiv of P^tBu_3 to **2a** produced a 2.5:1.0 equilibrium ratio of **2a** and P^tBu_3-ligated **2b**. The addition of 1 equiv of Q-phos to **2a** produced a 5:1 mixture of **2a** and Q-phos-ligated **2d**. Thus, the order of bond strengths of these three ligands to the arylpalladium(II) halide complexes is 1-AdP^tBu_2 > P^tBu_3 > Q-phos.

Addition of the classic hindered aromatic phosphine ligand P(*o*-tol)$_3$ revealed similar binding affinities of P(*o*-tol)$_3$ and the hindered alkylphosphines to Pd(II). The addition of 1 equiv of P(*o*-tol)$_3$ to **2a** produced a 1:1 ratio of 1-AdP^tBu_2-ligated **2a** and the P(*o*-tol)$_3$-ligated dimer, $\{[(o\text{-tol})_3P]Pd(Ph)(Br)\}_2$. In contrast, reaction of $Pd[P(o\text{-tol})_3]_2$ with P^tBu_3 generates $Pd[P^tBu_3]_2$ and free P(o-tol)$_3$ with no $Pd[P(o\text{-tol})_3]_2$ remaining.

2-Adamantyl complex **2c** was more stable than complexes **2a**, **2b**, **2d**, and the tri-*o*-tolylphosphine-ligated arylpalladium halide complexes. Reaction of **2a** with 1 equiv of 2-AdP^tBu_2 converted all of **2a** to **2c**. The reaction energy computed for this transformation, −2.1 kcal/mol at the BP86/ECP1 + ZPE level, is consistent with this observation. Similarly, the addition of 1 equiv of tricyclohexylphosphine to **2a** produced 0.5 equiv of $[(PCy_3)_2Pd(Ph)Br]$ and left 0.5 equiv of **2a** unreacted. A trace amount of $Pd[PCy_3]_2$ was formed. Addition of 2 equiv of PCy_3 to **2a** generated $[(PCy_3)_2Pd(Ph)Br]$ and free 1-AdP^tBu_2 as the only products observed by ^{31}P NMR spectroscopy.

Discussion

Rates of Oxidative Addition and Catalytic Couplings. The qualitative trends in rates of oxidative addition to the isolated PdL_2 complexes (L = tri-tertiaryalkylphosphine) correlated with the rates of reactions catalyzed by these palladium(0) complexes. For example, the oxidative addition of aryl bromides and chlorides to PdL_2 with L = P^tBu_3 or 1-AdP^tBu_2 required heating, and no coupling reactions at room temperature have been described with these PdL_2 complexes as catalyst. Workers at Tosoh reported the coupling of aryl halides and diarylamines at 100−120 °C using $Pd(P^tBu_3)_2$ generated in situ as catalyst.[52] Fu and Dai have reported Negishi cross-couplings of aryl and vinyl chlorides catalyzed by $Pd(P^tBu_3)_2$ at 100 °C,[53] and mechanistic studies on aryl halide aminations with $Pd(P^tBu_3)_2$ as catalyst were conducted at 95 °C.[54] Reactions catalyzed by palladium with P^tBu_3 as ligand at room temperature have been conducted with the combination of $Pd(dba)_2$ and 1 equiv of P^tBu_3[31,34,55] or with precursors that contain one P^tBu_3 ligand per palladium.[25]

Geometry of Arylpalladium(II) Complexes. The ability and means by which the various complexes can adopt a fully square-planar geometry dictate whether they become monomeric with two phosphine ligands, dimeric with one phosphine per metal, or monomeric with one phosphine ligand and a weak agostic interaction. The oxidative addition of aryl bromide to $Pd(PPh_3)_4$ produces the four-coordinate *trans*-$(PPh_3)_2Pd(Ar)(Br)$.[56] Addition of aryl bromide to $Pd[(P(o\text{-tol})_3]_2$ produces the dimeric,

(52) Yamamoto, T.; Nishiyama, M.; Koie, Y. *Tetrahedron Lett.* **1998**, *39*, 2367.
(53) Dai, C.; Fu, G. C. *J. Am. Chem. Soc.* **2001**, *123*, 2719.
(54) Alcazar-Roman, L. M.; Hartwig, J. F. *J. Am. Chem. Soc.* **2001**, *123*, 12905.
(55) Hartwig, J. F.; Kawatsura, M.; Hauck, S. I.; Shaughnessy, K. H.; Alcazar-Roman, L. M. *J. Org. Chem.* **1999**, *64*, 5575.
(56) Moser, W. R.; Wang, A. W.; Kjeldahl, N. K. *J. Am. Chem. Soc.* **1988**, *110*, 2816.

Table 5. A Comparison of the Bond Angles that Surround the Pd Atoms in {[(*o*-tol$_3$)P]Pd(Ar)(Br)} and **2a**

complex	Br–Pd–C_{ipso} (deg)	Br–Pd–P (deg)	P–Pd–C_{ipso} (deg)	smallest Pd–P–C angle
{[(*o*-tol$_3$)P]Pd(Ar)(Br)}$_2$	87.1(3)	174.7(9)	89.8(3)	109.5
(1-AdP^{t}Bu$_2$)Pd(Ph)(Br) (**2a**)	91.4(1)	162.61(3)	100.8(1)	106.0

four-coordinate complex {[(*o*-tol$_3$)P]Pd(Ar)(Br)}$_2$ with one phosphine per palladium,[18,19] while addition of aryl bromides to Pd(P^{t}Bu$_3$)$_2$ generates the monomeric complexes (P^{t}Bu$_3$)Pd(Ar)(Br). Both the monomeric PPh$_3$ complexes and the dimeric P(*o*-tol$_3$) complexes are square planar about the palladium atom. In contrast, the P^{t}Bu$_3$ complex contains a T-shaped orientation of the three heavy atoms bound to palladium. This complex could be considered square planar if an agostic hydrogen is included as the fourth ligand on palladium, but the geometry is distinct from complexes that adopt a four-coordinate geometry by coordinating the halide of a second arylpalladium halide fragment or a second phosphine ligand.

A comparison of the steric properties of P(*o*-tol)$_3$ and P^{t}Bu$_3$ and the geometries of the respective arylpalladium halide complexes reveals the factors that control the geometry and nuclearity of arylpalladium halide complexes. Since the time when Tolman reported that the cone angle of P(*o*-tol)$_3$ is 12° larger than the cone angle of P^{t}Bu$_3$,[57] alternative methods to measure these cone angles have been reported.[58] By solid angle measurements, the cone angle of P(*o*-tol)$_3$ is closer to 144° than to the 194° angle in Tolman's original report, but the cone angle of P^{t}Bu$_3$ was unchanged.

The weakness of the C−H agostic interaction in compounds **2** and **3** revealed by spectroscopic and computational studies and the potential for P(*o*-tol)$_3$ to adopt a smaller cone angle lead to the difference in structures of the complexes of the tertiary alkylphosphine ligands in this study and those of the hindered triarylphosphines. If the agostic interaction were stronger than the interaction with a bridging halide ligand, then complexes of P(*o*-tol)$_3$ could adopt a monomeric structure with an *ortho*-tolyl hydrogen occupying the open site. Although dimeric in their most stable form, the P(*o*-tol)$_3$ complexes often react through their monomeric form, and the monomer is likely to be stabilized by such a weak agostic interaction.

The steric factors that determine monomeric or dimeric structures are more subtle. Dimerization of the monomeric complexes in the current work would require substantial reorganizations and increased steric interactions. Selected angles from the structures of monomeric 1-AdP^{t}Bu$_2$Pd(Ph)(Br) **2a** and the dimeric complex {[(*o*-tol$_3$)P]Pd(Ar)(Br)}$_2$ determined by X-ray diffraction are shown in Table 5. The largest difference between the selected angles of the two complexes is the Br−Pd−P bond angle. The association of two monomeric **2a** species to form one dimeric complex would require the Br−Pd−P angle to increase by 12°, the P−Pd−C angle to decrease by 11°, and the phosphine to pivot back to a more conventional conformation with relatively equivalent Pd−P−C angles. Moreover, the open coordination site adopted by one of the *tert*-butylmethyl groups would be occupied by the bridging halogen. With three large substituents in roughly 3-fold symmetry, a bulky tertiaryalkyl phosphine ligand cannot adopt a conformation that avoids steric interactions with the other ligands of a planar, four-coordinate geometry.

Summary

This work has revealed a simple method to access a variety of arylpalladium(II) halide complexes with a novel coordination sphere by oxidative addition of aryl bromides and iodides to bis-phosphine palladium(0) complexes. This coordination sphere contains an aryl group, a halide, and only one phosphine ligand, along with a weak agostic interaction. In all cases, the aryl chloride and aryl triflate complexes could not be isolated by direct oxidative addition to the palladium(0) species but were prepared from the bromide by anion exchange. Structural studies of these compounds revealed the geometric distortions that occur to accommodate the bulky ligands and the origin of the preference for mononuclear versus dinuclear structures with a single ligand. Moreover, extensive computational studies have confirmed the presence of a weak agostic interaction between the metal and a ligand hydrogen that appeared in the solid-state structure but was revealed by spectroscopy in only one case. Because arylpalladium(II) halide complexes are proposed as intermediates in many cross-coupling reactions, studies on the rates of formation of these complexes and studies on the reactivity of these isolated species should provide insight into the mechanisms of metal-catalyzed cross-coupling processes.

Experimental Section

General Methods. ^{1}H and ^{13}C NMR spectra were recorded on a Bruker DPX 400 MHz spectrometer, Bruker DPX 500 MHz spectrometer, or a General Electric Omega 500 spectrometer with tetramethylsilane or residual protiated solvent used as a reference. Elemental analyses were performed by Robertson Microlabs, Inc., Madison, NJ. All ^{31}P and ^{13}C NMR spectra were proton decoupled. Toluene, tetrahydrofuran, ether, and pentane were distilled from sodium−benzophenone. Phenyl bromide was purified by distillation; however, the results were similar to those using phenyl bromide as received. Phenyl iodide, silver triflate, and tetraoctylammonium chloride were used without further purification. The syntheses of Pd[1-AdP^{t}Bu$_2$]$_2$,[12] Pd[P^{t}Bu$_3$]$_2$,[59] Pd[Q-phos]$_2$,[60] 1-AdP^{t}Bu$_2$,[61] 2-AdP^{t}Bu$_2$,[61] 2-AdP^{t}Bu$_2$Pd(Ph)Br (**2c**),[12] and P^{t}Bu$_3$Pd(*m*-xylyl)I (**3b**) [12] have been published previously.

1-AdP^{t}Bu$_2$Pd(Ph)Br (2a). In a glovebox, 540 mg (0.810 mmol) of Pd[1-AdP^{t}Bu$_2$]$_2$ (**1a**), 4.0 mL (38.0 mmol) of phenyl bromide, and a stir bar were added to a screw-capped vial. The vial was removed from the glovebox and heated at 70 °C for 2.5 h or until ^{31}P NMR spectroscopy showed complete consumption of **1**. The vial was returned to the drybox and added to a stirring flask filled with 50 mL of pentane. An orange precipitate formed immediately. The flask was stirred for 5 min. At this time, the orange precipitate was washed 5 × 10 mL with pentane. The orange solid was dried under vacuum to yield 70.2% (309 mg, 0.569 mmol) of the desired product. Spectroscopic data for this complex were published previously.

(57) Tolman, C. A. *Chem. Rev.* **1977**, *77*, 313.
(58) Brown, T. L.; Lee, K. J. *Coord. Chem. Rev.* **1993**, *128*, 89.
(59) Otsuka, S.; Yoshida, T.; Matsumoto, M.; Nakatsu, K. *J. Am. Chem. Soc.* **1976**, *98*, 5850.
(60) Shelby, Q.; Kataoka, N.; Mann, G.; Hartwig, J. F. *J. Am. Chem. Soc.* **2000**, *122*, 10718.
(61) Stambuli, J. P.; Stauffer, S. R.; Shaughnessy, K. H.; Hartwig, J. F. *J. Am. Chem. Soc.* **2001**, *123*, 2677.

1-AdP^{t}Bu$_2$Pd(Ph)I (3a). In a glovebox, an NMR tube was charged with 102 mg (0.153 mmol) of Pd[1-AdP^{t}Bu$_2$]$_2$ (**1**) and 1.0 mL (8.9 mmol) of phenyl iodide. The tube was heated at 70 °C for 7 min or until ^{31}P NMR spectroscopy showed complete consumption of **1a**. The tube was returned to the drybox and added to a vial filled with 20 mL of pentane. An orange precipitate was immediately formed. The vial was stirred for 5 min. At this time, the orange precipitate was washed 5 × 5 mL with pentane. The orange solid was dried under vacuum to yield 87% (79 mg, 0.13 mmol) of the desired product. The product decomposed in solution after 1 h. ^{1}H NMR (CD_2Cl_2, 500 MHz, 0 °C): δ 1.44 (d, J = 12.5 Hz, 18H), 1.74−1.80 (br m, 6H), 2.04 (br s, 3H), 2.21 (br s, 6H), 6.79−6.83 (m, 1H), 6.85−6.88 (m, 2H), 7.24 (d, J = 6.5 Hz, 2H). ^{13}C NMR{^{1}H} (CD_2Cl_2, 500 MHz, 0 °C): δ 29.0 (d, J = 7.8 Hz), 32.4 (d, J = 2.1 Hz), 41.1 (d, J = 7.6 Hz), 41.4, 49.2 (d, J = 7.1 Hz), 123.8, 127.0 (d, J = 2.5 Hz), 132.9 (d, J = 6.4 Hz), 136.6 (d, J = 3.9 Hz). ^{31}P NMR (C_6D_6, 202 MHz): δ 50.6.

1-AdP^{t}Bu$_2$Pd(Ph)CF$_3$SO$_3$ (5a). In a glovebox, 98 mg (0.18 mmol) of 1-AdP^{t}Bu$_2$Pd(Ph)Br (**2a**) was dissolved in 2 mL of toluene and stirred. In a separate vial, silver triflate (57 mg, 0.22 mmol) was dissolved in 2 mL of toluene. The silver triflate solution was added dropwise to the stirring vial, whose appearance changed from a clear orange solution to a cloudy dark green mixture. The reaction was stirred for an additional 2 min. At this time, the reaction mixture was filtered through a plug of Celite and concentrated to approximately 1 mL. The resulting bright yellow solution was layered with pentane and cooled to −35 °C. After 12 h, bright yellow crystals formed that were washed with 5 mL of pentane and dried under vacuum to yield 78% (87 mg, 0.14 mmol) of the desired product. ^{1}H NMR (C_6D_6, 500 MHz): δ 1.03 (d, J = 13.0 Hz, 18H), 1.41−1.55 (br m, 6H), 1.74 (br s, 3H), 1.98 (br s, 6H), 6.79−6.81 (m, 3H), 7.28−7.31 (m, 2H). ^{13}C NMR{^{1}H} (C_6D_6, 125 MHz): δ 29.0 (d, J = 7.3 Hz), 32.1 (d, J = 1.9 Hz), 36.1, 40.7 (d, J = 12.4 Hz), 41.4, 48.8 (d, J = 10.8 Hz), 125.7, 128.2 (br s), 135.3 (d, J = 5.8 Hz), 135.4 (d, J = 2.1 Hz). ^{31}P NMR (C_6D_6, 202 MHz): δ 72.1. Anal. Calcd for $C_{25}H_{38}F_3O_3PPdS$: C, 48.98; H, 6.25. Found: C, 48.59; H, 5.87.

P^{t}Bu$_3$Pd(Ph)Br (2b). In a glovebox, 293 mg (0.574 mmol) of Pd[P^{t}Bu$_3$]$_2$ (**7**), 2.8 mL of phenyl bromide (26 mmol), and a stir bar were added to a screw-capped vial. The vial was removed from the glovebox and heated at 70 °C for 2.5 h or until ^{31}P NMR spectroscopy showed complete consumption of **1b**. The vial was returned to the drybox and added to a stirring flask filled with 30 mL of pentane. An orange precipitate was immediately formed. The flask was stirred for 5 min. At this time, the orange precipitate was washed 5 × 10 mL with pentane. The orange solid was dried under vacuum to yield 64% (170 mg, 0.365 mmol) of the desired product. ^{1}H NMR (C_6D_6, 400 MHz): δ 1.00 (d, J = 12.8 Hz, 27H), 6.74 (t, J = 7.2 Hz, 1H), 6.82 (t, J = 7.2 Hz, 2H), 7.43 (m, 2H). ^{13}C NMR{^{1}H} (C_6D_6, 125 MHz): δ 32.1, 40.2 (d, J = 8.4 Hz), 124.0, 127.2, 129.0, 137.0 (d, J = 3.0 Hz). ^{31}P NMR (C_6D_6, 202 MHz): δ 63.0. Anal. Calcd for $C_{18}H_{32}BrPPd$: C, 46.42; H, 6.93. Found: C, 46.20; H, 6.84.

Q-phos Pd(Ph)Br (2d). In a glovebox, 60 mg (0.039 mmol) of Pd[Q-phos]$_2$ (**1c**), 0.17 mL of phenyl bromide (1.6 mmol), 2.7 mL of THF, and a stir bar were added to a screw-capped vial. The vial was stirred in the glovebox for approximately 2.5 h or until ^{31}P NMR spectroscopy showed complete consumption of **1c**. The red solution was evaporated until all of the THF was removed. At this time, approximately 15 mL of pentane was added, and the vial was shaken and cooled at −35 °C. The vial was removed from the freezer, and the red precipitate that formed was washed repeatedly with ether until all of the free ligand was removed (as judged by ^{1}H NMR spectroscopy). The solid was dissolved in a minimal amount of THF. Ether was added until the clear red solution became cloudy. After cooling to −35 °C for 26 h, red crystals appeared in the vial. The red crystals were washed with pentane (1 × 5 mL) and dried under vacuum to yield 29% (11 mg, 0.0.011 mmol) of the desired product. ^{1}H NMR (C_6D_6, 500 MHz): δ 1.03 (d, J = 14.0 Hz, 18H), 4.55 (s, 2H), 4.77 (s, 2H), 6.88−6.93 (br m, 3H), 7.20−7.22 (br m, 17H), 7.26−7.28 (br m, 10H). ^{13}C NMR{^{1}H} (CD_2Cl_2, 100 MHz): δ 30.5 (d, J = 3.6 Hz), 39.0 (d, J = 17.2 Hz), 76.7 (25.9 Hz), 78.4 (d, J = 7.0 Hz), 80.1 (d, J = 7.7 Hz), 88.8, 124.6, 126.7, 127.4, 128.2, 132.9, 133.3, 135.4, 135.8 (d, J = 2.6 Hz). ^{31}P NMR (C_6D_6, 202 MHz): δ 49.2. Anal. Calcd for $C_{54}H_{52}$-PPdBrFe: C, 66.58; H, 5.38. Found: C, 66.18; H, 5.32.

Q-phos Pd(Ph)I (3d). Complex **3c** was prepared in a manner similar to **2c** to give 75.4% (0.0492 mmol, 50.2 mg) of a red powder. ^{1}H NMR (CD_2Cl_2, 400 MHz): δ 1.03 (d, J = 14.0 Hz, 18H), 4.54 (s, 2H), 4.74 (s, 2H), 6.84−6.89 (br m, 3H), 7.12−7.25 (br m, 27H), 7.26−7.28. ^{13}C NMR{^{1}H} (CD_2Cl_2, 100 MHz): δ 30.5 (d, J = 4.2 Hz), 39.1 (d, J = 16.4 Hz), 77.1 (d, J = 22.9 Hz), 78.1 (d, J = 7.4 Hz), 79.9 (d, J = 5.8 Hz), 88.8, 124.4, 127.3, 128.2, 132.1 (d, J = 5.5 Hz), 132.9, 133.3, 135.4, 136.0 (d, J = 4.1 Hz). ^{31}P NMR (C_6D_6, 202 MHz): δ 45.7.

Synthesis of the Phosphonium Salt [Q-phos(Ph)]$^+$[OTf]$^-$. In a glovebox, 102 mg (0.066 mmol) of Pd[Q-phos]$_2$ (**1c**), 0.40 mL of phenyl triflate (2.5 mmol), 9.0 mL of THF, and a stir bar were added to a screw-capped vial. The vial was stirred at 60 °C for approximately 2 h or until ^{31}P NMR spectroscopy showed complete consumption of **1c**. The dark brown solution was evaporated until all of the THF was removed. The vial was removed from the glovebox, and 20 mL of benzene was added. The benzene solution was filtered through a glass-fritted funnel, and the filtrate was allowed to slowly evaporate at 23−25 °C. After 16 h, the filtrate was decanted to reveal purple crystals, which were washed with cold benzene and dried under vacuum to yield 75% (47 mg, 0.050 mmol) of the desired product. ^{1}H NMR (CD_2Cl_2, 500 MHz): δ 1.32 (d, J = 16.0 Hz, 18H), 4.99 (br s, 4H), 7.08−7.19 (m, 22H), 7.24−7.26 (m, 5H), 7.66−7.68 (m, 1H), 8.17−8.20 (m, 2H). ^{13}C NMR{^{1}H} (CD_2Cl_2, 125 MHz): δ 29.0, 38.5 (d, J = 36.6 Hz), 79.7 (d, J = 8.6 Hz), 83.2 (d, J = 9.1 Hz), 88.5, 128.0, 128.2, 128.3, 130.1 (d, J = 11.7 Hz), 132.9, 134.2, 135.3, 135.4. ^{31}P NMR (CH_2Cl_2, 202 MHz): δ 53.5. Anal. Calcd for $C_{55}H_{52}F_3FeO_3PS$: C, 70.51; H, 5.59. Found: C, 70.47; H, 5.47.

Independent Synthesis of [(PCy$_3$)$_2$Pd(Ph)(Br)]. In a drybox, Pd(PCy$_3$)$_2$ (232 mg, 0.348 mmol), phenyl bromide (55 uL, 0.52 mmol), and 2 mL of benzene were stirred at 25 °C for 24 h. At this time, the white solid that precipitated from the reaction was collected by filtration. The white solid was crystallized from cold ether to yield 58% (165 mg, 0.200 mmol) of the title compound. ^{1}H NMR (C_6D_6, 500 MHz): δ 1.11−1.22 (br s, 18H), 1.59−1.76 (m, 30H), 2.07−2.09 (m, 12H), 2.29 (br s, 6H), 6.87 (t, J = 7.0 Hz, 1H), 6.87 (t, J = 7.0 Hz, 2H), 7.59 (d, J = 7.0 Hz, 2H). ^{13}C NMR{^{1}H} (C_6D_6, 125 MHz): δ 27.0, 28.0 (t, J = 4.0 Hz), 30.6, 34.7 (t, J = 9.4 Hz), 122.2, 127.5, 138.9 (t, J = 3.0 Hz), 155.2 (br s). ^{31}P NMR (C_6D_6, 202 MHz): δ 20.6 Anal. Calcd for $C_{42}H_{71}P_2BrPd$: C, 61.20; H, 8.68. Found: C, 60.97; H, 8.64.

Computational Details. Molecular structures have been fully optimized at the BP86/ECP1 level, i.e., employing the exchange and correlation functionals of Becke and Perdew,[62−64] respectively, together with a fine integration grid (75 radial shells with 302 angular points per shell), relativistic MEFIT effective core potentials with the corresponding valence basis sets for Pd[65] (contraction schemes [6s5p3d]), and standard 6-31G* basis set[66,67] for all other elements. The nature of each stationary point was characterized by analytical calculation of the harmonic vibrational frequencies at that level. Nuclear magnetic shieldings σ have been evaluated for the BP86/ECP1 geometries using a recent implementation of the gauge-including atomic orbitals (GIAO)-DFT method,[68] involving the functional combinations according to Becke (hybrid) and Lee, Yang, and Parr[69,70] (B3LYP), together with

(62) Becke, A. D. *Phys. Rev. A* **1988**, *38*, 3098.
(63) Perdew, J. P. *Phys. Rev. B* **1986**, *33*, 8822.
(64) Perdew, J. P. *Phys. Rev. B* **1986**, *34*, 7406.
(65) Andrae, D.; Häussermann, U.; Dolg, M.; Stoll, H.; Preuss, H. *Theor. Chim. Acta* **1990**, *77*, 123.
(66) Hehre, W. J.; Ditchfield, R.; Pople, J. A. *J. Chem. Phys.* **1972**, *56*, 2257.
(67) Hariharan, P. C.; Pople, J. A. *Theor. Chim. Acta* **1973**, *28*, 213.

basis II″, i.e., a [16s10p9d] all-electron basis for Pd, contracted from the well-tempered 22s14p12d set of Huzinaga and Klobukowski[71] and augmented with two d-shells of the well-tempered series, the recommended IGLO-basis II[72,73] on the three donor atoms bonded to Pd, the nearest CH moiety (without f-functions on the halogens), and a double-ζ basis[72] on all other atoms.[74] Chemical shifts δ have been calculated relative to TMS computed at the same level ($\sigma(^1H) = 31.7$). These computations were performed using the Gaussian 98 program package.[75] Topological analysis of the charge density (Bader analysis)[48] has been performed at the BP86/ECP1 level using the Morphy program.[76]

Acknowledgment. We are grateful to the NIH-NIGMS (GM58108) for support of this work. We thank Merck Research Laboratories for an unrestricted gift and Johnson-Matthey for a gift of $PdCl_2$. M.B. thanks Prof. W. Thiel and the Deutsche Forschungsgemeinschaft for support.

Supporting Information Available: Crystallographic data for **5a**, **2b**, and **2d** as well as NMR spectra for **3a** (PDF and CIF). This material is available free of charge via the Internet at http://pubs.acs.org.

JA037928M

(68) Cheeseman, J. R.; Trucks, G. W.; Keith, T. A.; Frisch, M. J. *J. Chem. Phys.* **1996**, *104*, 5497.
(69) Becke, A. D. *J. Chem. Phys.* **1993**, *98*, 5648.
(70) Lee, C.; Yang, W.; Parr, R. G. *Phys. Rev. B* **1988**, *37*, 785.
(71) Huzinaga, S.; Klobukowski, M. *J. Mol. Struct.* **1988**, *167*, 1.
(72) Kutzelnigg, W.; Fleischer, U.; Schindler, M. *NMR Basic Principles and Progress*; Springer-Verlag: Berlin, 1990; Vol. 23.
(73) Fleischer, U. Bochum, Germany, 1992.
(74) Bühl, M.; Sassmannshausen, J. *J. Chem. Soc., Dalton Trans.* **2001**, 79.
(75) Frisch, M. J.; Trucks, G. W.; Schlegel, H. B.; Scuseria, G. E.; Robb, M. A.; Cheeseman, J. R.; Zakrzewski, V. G.; Montgomery, J. A., Jr.; Stratmann, R. E.; Burant, J. C.; Dapprich, S.; Millam, J. M.; Daniels, A. D.; Kudin, K. N.; Strain, M. C.; Farkas, O.; Tomasi, J.; Barone, V.; Cossi, M.; Cammi, R.; Mennucci, B.; Pomelli, C.; Adamo, C.; Clifford, S.; Ochterski, J.; Petersson, G. A.; Ayala, P. Y.; Cui, Q.; Morokuma, K.; Malick, D. K.; Rabuck, A. D.; Raghavachari, K.; Foresman, J. B.; Cioslowski, J.; Ortiz, J. V.; Stefanov, B. B.; Liu, G.; Liashenko, A.; Piskorz, P.; Komaromi, I.; Gomperts, R.; Martin, R. L.; Fox, D. J.; Keith, T.; Al-Laham, M. A.; Peng, C. Y.; Nanayakkara, A.; Gonzalez, C.; Challacombe, M.; Gill, P. M. W.; Johnson, B. G.; Chen, W.; Wong, M. W.; Andres, J. L.; Head-Gordon, M.; Replogle, E. S.; Pople, J. A. *Gaussian 98*, revision A.11.1; Gaussian, Inc.: Pittsburgh, PA, 1998.
(76) Popelier, P. L. A. *Comput. Phys. Commun.* **1996**, *93*, 212.